Results for binary fluid mixtures of carbon dioxide with large molecular size hydrocarbons [e.g. 2,6,10,15,19,23-hexamethyltetracosane (perhydrosqualene, squalane), squalene] and some alcohols (e.g. 2-hexanol, 2-octanol, 2,5-hexanediol) in the temperature range −20 to +200°C at up to 1 kbar are presented and compared to earlier data on CO_2 binaries with alkanes up to hexadecane [*Chem.-Ing.Tech.*, **39**, 649 (1967)]. Whereas CO_2–2-hexanol and CO_2–2-octanol resemble CO_2–octane and exhibit critical liquid–liquid and liquid–gas phenomena that do not intersect in the three-dimensional pressure–temperature–composition space, for CO_2–squalane and CO_2–squalene the liquid–liquid and liquid–gas critical curves are superimposed, as found earlier for the CO_2–hexadecane system. For CO_2–squalane the critical curve runs through a temperature minimum at (55 ± 0·5)°C and (705 ± 20) bars and then rises steeply to higher pressures with increasing temperatures; thus its phase behaviour resembles that of systems that exhibit gas–gas equilibria of the second type [*J. Chem. Thermodyn.*, 7, 805 (1975)]. Additional results on binary mixtures of ethane with methanol, 2,5-hexanediol, and nitromethane show that all these systems resemble the CO_2–squalane type. Practical applications for industrial extractions and separation methods, e.g. supercritical fluid chromatography are briefly discussed.

Earlier measurements of phase equilibria and critical phenomena in fluid mixtures of water with hydrocarbons [see *Ber. Bunsenges. Phys. Chem.*, 71, 633 (1967); 73, 294 (1969); 74, 682 (1970)] were extended to aqueous solutions of fluorocarbons. Results are presented for the system water–fluorobenzene in the temperature range 300 to 360°C at up to 3·5 kbar; from the measurements parts of the critical curves were determined. The results show that the critical curve of this system has a similar shape to that for the CO_2–squalane system. It is quite astonishing that the critical $p(T)$ curve of this system nearly coincides with that of the water–benzene system measured earlier.

All results are discussed in relation to data on related systems reported in the literature. They show that a whole pattern of transition types between liquid–gas, liquid–liquid and gas–gas equilibria exists, confirming thus earlier attempts to explain the phase separation effects in fluid mixtures at high pressures on the basis of phase-theoretical arguments [for a review see G. M. Schneider, *Pure Appl. Chem.*, **47**, 277 (1976); G. M. Schneider in *Chemical Thermodynamics* (Chemical Society Specialist Periodical Report), volume 2, in the press].

Phase diagrams of NH_4I and NH_4Br from Raman measurements at high pressure

W Gebhardt, T Geisel, H D Hochheimer, E Spanner
University of Regensburg, Regensburg, BRD/West Germany

We report on the Raman spectra of the three CsCl-type phases of NH_4Br and NH_4I which differ in the orientations of the NH_4 tetrahedra. The two possible orientations are randomly occupied in phase II (O_h symmetry). The tetrahedra are all equally oriented in phase IV (T_d symmetry). In the tetragonal phase III neighbouring tetrahedra are equally oriented along the tetragonal axis and alternately along the other Cartesian axes (D_{4h} symmetry). The Raman spectra of the three phases differ sharply. Owing to disorder in phase II all phonons may contribute more or less to the Raman spectra. The D_{4h} symmetry of phase III bisects the Brillouin zone of the CsCl-type lattice. Only M point modes of this Brillouin zone and the libration ν_6 can be observed in this phase (figure 1). In the T_d symmetry of phase IV strong scattering from the TO (Γ) mode is observed, whereas the intensity of the other

bands, LO (Γ), LA (M), and TA (M), is weak. The TA (M) and LA (M) bands are due to residual disorder. The libration ν_6 is forbidden by symmetry but the second harmonic $2\nu_6$ is allowed. In the phase diagram for NH_4I derived from these measurements the triple point is found at higher pressure than in the diagrams of Zlunitsyn (1938, 1939) and of Stevenson (1961) (figure 2).

Special attention was given to the possible occurrence of a fifth phase in NH_4Br as reported by Garland and Young (1968) and more recently by Ebisuzaki (1973)

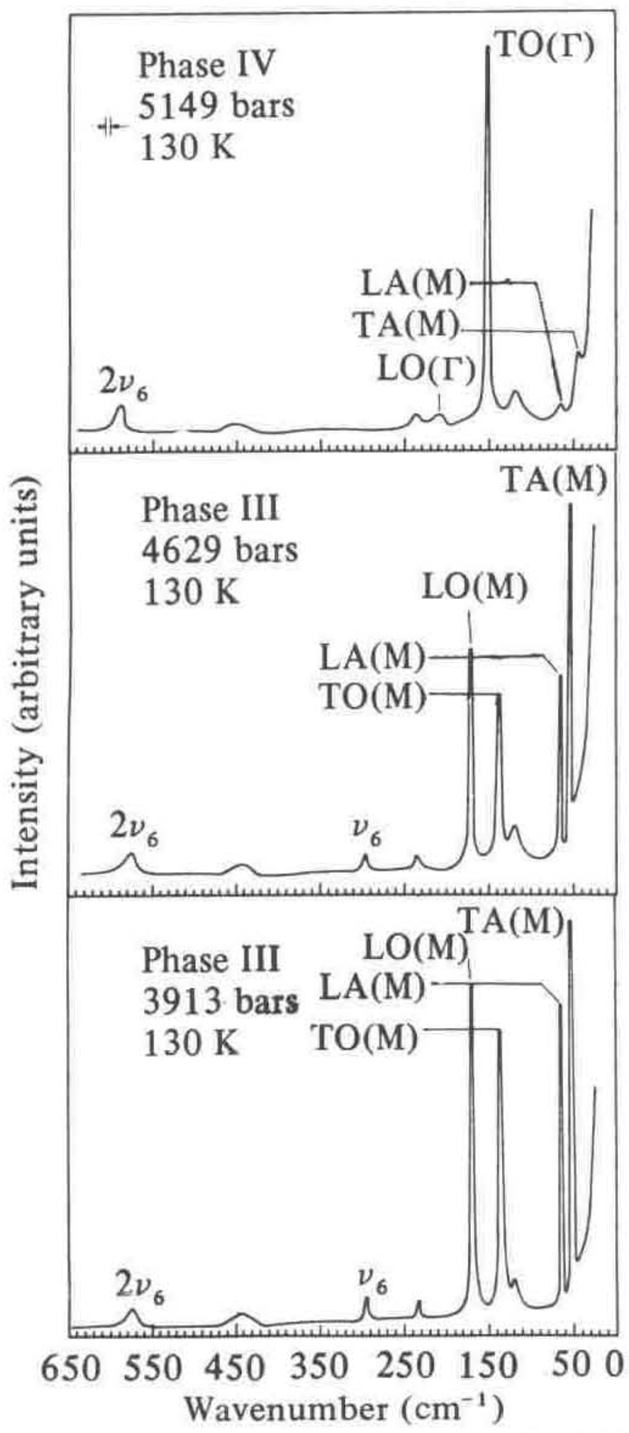

Figure 1. Raman spectra of NH_4I at three different pressures.

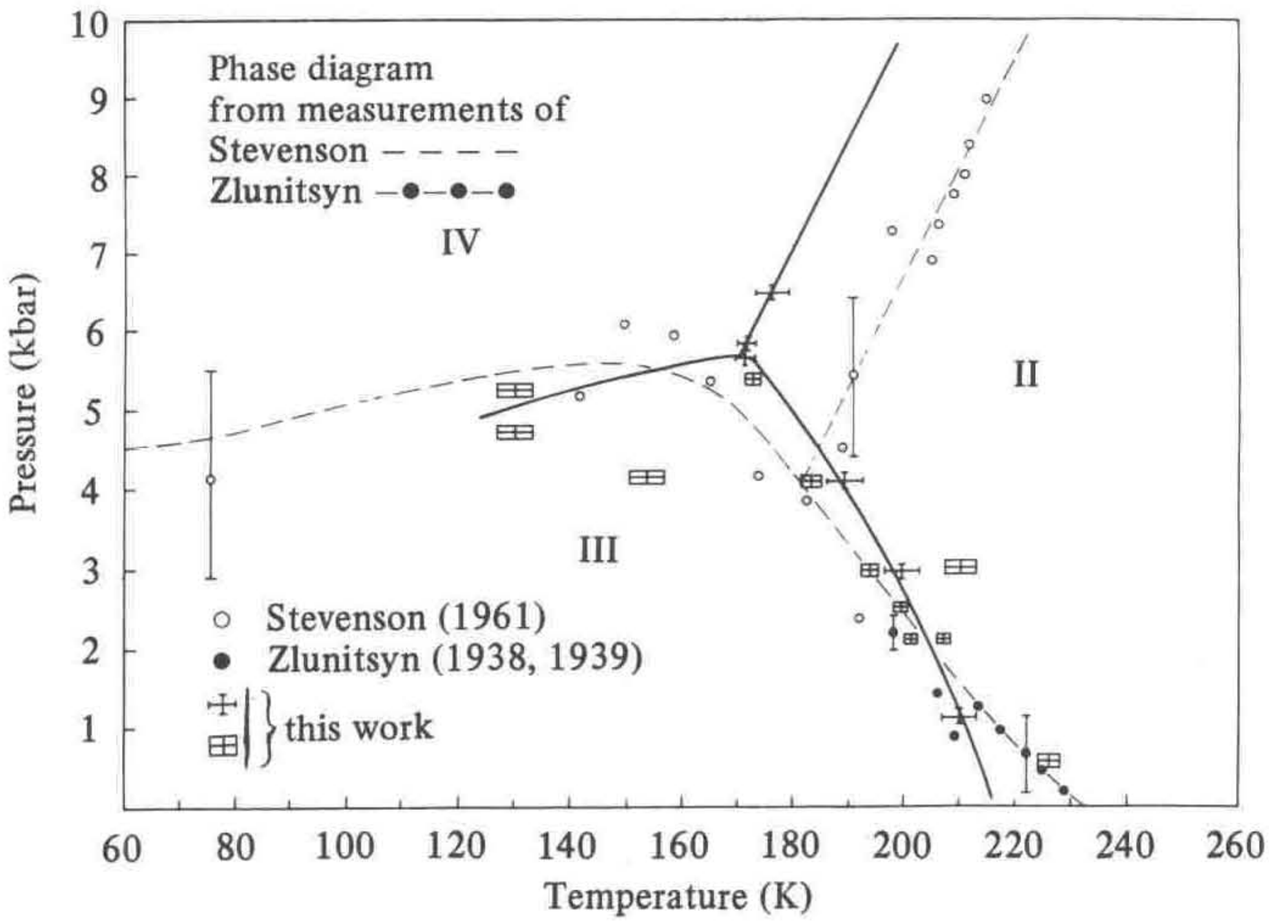

Figure 2. Phase diagram of NH_4I. The crosses mark the uncertainty of the phase line. The crossed rectangles give the range of measurement with unique phase determination.

and Wang and Wright (1974). We calculated the Raman spectra of phase IV and of the two suggested structures of phase V (Garland and Young, 1968) using the method proposed by Geisel and Keller (1975). A further phase transition IV ⇌ V, which should be accompanied by changes in the frequencies or intensities of Raman bands, is not observed (figure 3). Comparison of the calculated spectra with our measurements and with those reported by Ebisuzaki (1973) and Wang and Wright (1974) shows that, in the P, T range where phase V was expected, actually only phase IV was observed.

The Raman scattering experiment was performed in a high-pressure He cell kept in a temperature controlled cryostat. Near the triple point in NH_4I a hysteresis between 3–4 K and 100–200 bars was found.

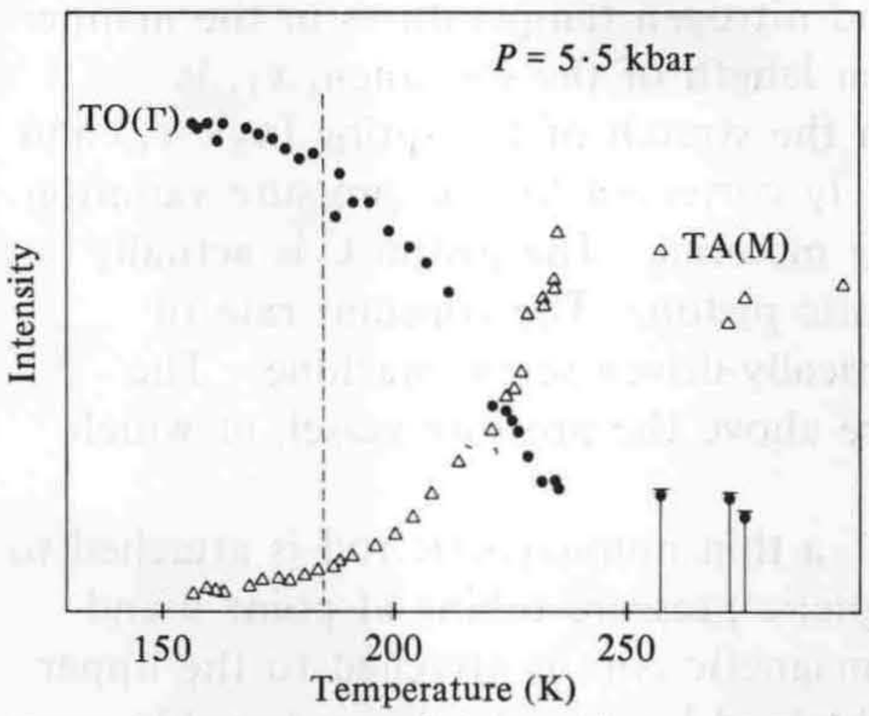

Figure 3. Variation of the scattering intensities of two modes in NH_4Br at 5·5 kbar. The dashed vertical line shows the suggested IV ⇌ V phase transition which was not observed.

References

Ebisuzaki, Y., 1973, *Chem. Phys. Lett.*, **19**, 503.
Garland, C. W., Young, R. H., 1968, *J. Chem. Phys.*, **49**, 5282.
Geisel, T., Keller, J., 1975, *J. Chem. Phys.*, **62**, 3777.
Stevenson, R., 1961, *J. Chem. Phys.*, **34**, 1757.
Wang, C. H., Wright, R. B., 1974, *J. Chem. Phys.*, **61**, 339.
Zlunitsyn, S. A., 1938, *Zh. Eksp. Teor. Fiz.*, **8**, 724.
Zlunitsyn, S. A., 1939, *Zh. Eksp. Teor. Fiz.*, **9**, 72.

Elastic scaling parameters in the yield stress of metals

A L Ruoff, J O Chua
Department of Materials Science and Engineering, Cornell University, Ithaca, New York 14853 USA

If the yield stress of a metal is determined solely by the motion of screw dislocations in an isotropic medium, it is expected to vary with pressure according to

$$\sigma_0 = \sigma_{00}\left(1+\frac{G_0' P}{G_0}\right), \tag{1}$$

inasmuch as

$$G = G_0\left(1+\frac{G_0'}{G_0}P\right) \tag{2}$$

accurately represents the pressure variation of $G(P)$. Here σ_{00} is the yield stress at zero pressure, G_0 is the shear modulus at zero pressure, and G_0' is the pressure derivative of the shear modulus evaluated at zero pressure. If edge dislocations only

are involved instead, we expect

$$\sigma_0 = \sigma_{00}\left(1+\frac{C_0^{e'}}{C_0^{e}}P\right) \tag{3}$$

where $C^e = G/(1-\nu)$, with ν being Poisson's ratio.

In order to observe the pressure variation of the yield stress of metals we have (i) constructed a device capable of accurately measuring the stress–strain curve at pressure, and (ii) chosen a metal with a small shear modulus, since it is known that the pressure derivative is approximately the same for all materials. Potassium was therefore chosen. The bulk shear modulus for potassium at liquid nitrogen temperature is only 20·8 kbar (this should be compared with the value of 828 kbar for steel at room temperature).

The stress–strain curve was obtained at liquid nitrogen temperatures in the manner shown schematically in figure 1. The change in length of the specimen, x_1, is directly measured. The force is obtained from the stretch of the spring (x_2-x_1) and the known spring constant which is appropriately corrected for the pressure variation of the moduli and the dimensions of the spring material. The piston C is actually high-pressure tubing which slides within the static piston. The constant rate of motion of this piston is controlled by an electrically-driven screw machine. The hollow piston C extends a considerable distance above the pressure vessel, at which point the tubing is sealed.

The displacement x_1 is measured as follows: a thin nonmagnetic rod is attached to the grip at point a and passes into the nonmagnetic pressure tubing at point b and extends upward above the pressure vessel. A magnetic core is attached to the upper end of this rod. The position of the core is obtained by use of a linear variable differential transformer (LVDT) placed over the pressure tubing at atmospheric pressure. This technique has previously been used in making high pressure creep studies (Butcher *et al.*, 1964) and equation-of-state studies (Lincoln and Ruoff, 1973). The displacement x_2 is also measured with the use of an LVDT system. The combined

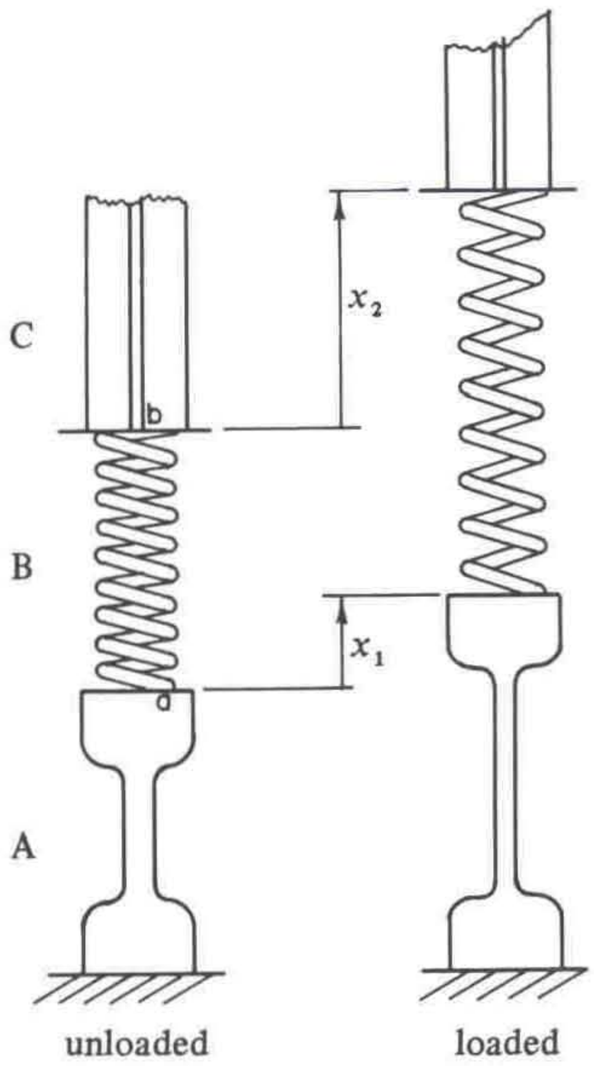

Figure 1. Schematic diagram of the measuring device. A specimen in grips; B spring; C nonmagnetic moving hollow piston. The thin rod which extends from point a into the hollow tube and which holds the magnetic core is not shown.